ARCHIVES OF MECHANICS
Arch. Mech. **74** (6), 549–564, 2022, DOI: 10.24423/aom.4013

Stokes flow in lid-driven cavity under inclined magnetic field

M. GÜRBÜZ-ÇALDAĞ[1,2], E. ÇELİK[3]

[1] *Başkent University, Department of Management, Ankara, Turkey, e-mail: mervegurbuz@baskent.edu.tr (corresponding author)*

[2] *TED University, Department of Mathematics, Ankara, Turkey, e-mail: merve.gurbuz@tedu.edu.tr*

[3] *Çanakkale Onsekiz Mart University, Department of Computer Technologies, Çanakkale, Turkey, e-mail: e.celik@comu.edu.tr*

Stokes flow in a lid-driven cavity under the effect of an inclined magnetic field is studied. The radial basis function (RBF) approximation is employed to the magnetohydrodynamic (MHD) equations which include Navier–Stokes equations of fluid dynamics and Maxwell's equations of electromagnetics through Ohm's law with the Stokes approximation. Numerical results are obtained for the moderate Hartmann number ($0 \leq M \leq 80$) and different angles of a magnetic field ($0 \leq \alpha \leq \pi$). It is found that the increase in the Hartmann number causes the development of new vortices under the main flow due to the impact of a magnetic field. However, the type of the inclination angle (acute or obtuse) determines the location of the vortices.

Key words: radial basis function, MHD Stokes flow, inclination angle.

1. Introduction

Magnetohydrodynamics (MHD) deals with the flow of electrically conducting fluids under an applied magnetic field. MHD has wide range of industrial applications such as nuclear fusion, MHD pump, MHD generators [1] so that many researchers have used numerical methods to MHD flow problems. The boundary element method (BEM) [2–4] has been applied to MHD flow equations for moderate Hartman number values to analyze the effect of a magnetic field on the flow behaviour. In addition, the impact of the inclined magnetic field on MHD duct flow is analyzed by many researchers since the orientation of the magnetic field significantly influences the flow rates and pressure drops [5, 6]. Xiao and Kim [6] utilized the comercial code CFX to find the solution of MHD duct flow for the inclination angles $\alpha = 0, \pi/6, \pi/4, \pi/3$. They found that as the angle of a magnetic field increases, the mass flux goes up significantly. Hua and Walker [7] examined the effect of an inclined magnetic field on liquid metal in a rectangular duct. They solved MHD equations in terms

of pressure and electric potential for different values of the inclination angle. JEYANTHI and GANESH [8] employed the radial basis function generating the finite difference method (RBF-FD) to MHD duct flow with an obstacle. The numerical results were obtained for different values of the Hartmann number ($M = 10, 100$) and the inclination angle of the magnetic field ($0 \leq \theta \leq \pi/2$). They found that the increase in the Hartmann number decreases the magnitude of the velocity.

MHD flow in a lid-driven problem has attracted great attention due to its applications including crystal growth, solidification processing and so on. KEFAYATI *et al.* [9] employed the lattice Boltzmann method to MHD equations for different values of the Hartmann number and the Richardson number. They reported that heat transfer reduces as the Hartmann number increases. JIN *et al.* [10] studied three-dimensional flow in a driven-cavity subjected to magnetic field. They found that the magnetic field affects the circulation of the cavity. Moreover, the impact of an inclined magnetic field on the mixed convection flow has been analyzed by YU *et al.* [11]. Heat transfer was shown to be influenced by the orientation of the magnetic field. HUSSAIN *et al.* [12] implemented the finite element method to convection flow under an inclined magnetic field. They observed that the average Nusselt number decreases with an increasing Hartmann number. CHO [13] numerically simulated the effects of the inclined magnetic field on convection flow by taking the Hartmann number up to 50 and the inclination angle up to 2π. HUSSAIN *et al.* [14] examined the impacts of fins and inclined magnetic field on convection flow in a lid-driven cavity. They observed that the average Nusselt number values are dropped by increasing the number of adiabatic fins.

Stokes flow is highly viscous so that the governing equations are obtained from the Navier–Stokes equations neglecting the convection terms. Many researchers have analyzed the Stokes flow behaviour in cavities by using several techniques. YOUNG *et al.* [15] and CHEN *et al.* [16] applied the method of fundamental solutions (MFS) to Stokes flow. In [17], MFS has been developed for 2D and 3D Stokes problems to find velocity components and pressure. ELDHO and YOUNG [18] implemented the dual reciprocity boundary element method (DRBEM) to Navier–Stokes equations by taking the small Reynolds number. They showed that DRBEM provides accurate results. BUSTAMANTE *et al.* [19] considered Stokes flow in a lid-driven cavity and the backward facing step channel. They obtained numerical results by using a method of the approximate particular solution for different values of shape parameters. DELICEOĞLU and AYDIN [20] and ÇELIK *et al.* [21] investigated the flow patterns by using an analytical solution of the biharmonic equation ($\nabla^4\psi = 0$) of Stokes flow and analyzed the structures in view of topological aspects in an L-shaped and a Z-shaped cavity, respectively.

The effect of the uniform magnetic field on Stokes flow can be used to design MHD-based microfluidic devices such as micro-pumps, microcoolers, etc. [22]. YOSINOBU and KAKUTANI [23] studied MHD Stokes flow and obtained expansion formula in terms of the Hartmann number. GÜRBÜZ and TEZER-SEZGIN [24] implemented radial basis function approximation to MHD convection flow equations by taking Re = 0.6 (Stokes approximation). They analyzed the influence of the viscous dissipation, buoyancy force and horizontally applied magnetic field on Stokes flow. TÜRK [25] investigated the solution of the eigenvalue problem for MHD Stokes flow by using a spectral collocation method. Flattening tendency for velocity profiles was observed as the Hartmann number increases. PRASAD and BUCHA [26] examined the magnetic effect on creeping flow in a permeable spheroid with a solid core. They found that the drag force acting on permeable and semipermeable spheroids with an impermeable core under the MHD effect is higher as compared to the case without magnetic forces.

Based on the above literature survey and authors' knowledge, the impact of the inclined magnetic field on Stokes flow has never been studied. The main aim of this paper is to analyze the effect of the Hartmann number and orientation angle of the magnetic field on Stokes flow in a lid-driven cavity. The MHD Stokes flow equations are solved by the radial basis function (RBF) approximation which is the popular meshless method for the researches due to less computational cost. Also, the velocity disribution is used to handle the corner singularities and to obtain smooth eddies at the corners. Numerical results are depicted in terms of streamlines for several values of the Hartmann number ($0 \leq M \leq 80$) and inclination angle ($0 \leq \alpha \leq \pi$). It is found that both strength and the direction of the magnetic field control the behaviour of the Stokes flow. Moreover, a stream function magnitude decreases with the augmentation of an acute angle. While the increment of an obtuse angle α causes the magnitude of the stream function to increase.

2. Governing equations

The steady, fully developed flow of a viscous, incompressible and electrically conducting fluid is considered in a square cavity with a movement of the top wall. The uniform magnetic field is applied with an inclination angle α according to x-axis. MHD equations are governed by the Navier–Stokes equations and Maxwell's equations [23]. The non-dimensional equations in terms of velocity (u, v) and pressure p are:

$$\frac{\partial u}{\partial x} + \frac{\partial v}{\partial y} = 0, \tag{2.1}$$

$$\nabla^2 u = \mathrm{Re}\left(u\frac{\partial u}{\partial x} + v\frac{\partial u}{\partial y}\right) + \frac{\partial p}{\partial x} - M^2(-u\sin^2\alpha + v\sin\alpha\cos\alpha), \tag{2.2}$$

$$\nabla^2 v = \mathrm{Re}\left(u\frac{\partial v}{\partial x} + v\frac{\partial v}{\partial y}\right) + \frac{\partial p}{\partial y} - M^2(-v\cos^2\alpha + u\sin\alpha\cos\alpha). \tag{2.3}$$

The above equations are obtained by using non-dimensional variables $x \to xl$, $y \to yl$, $u \to uu_l$, $v \to vu_l$, $p \to p\rho\nu u_l/l$. The non-dimensional parameters are the Hartmann number $M = l\mu H_l(\sigma/\rho\nu)^{1/2}$ and the Reynolds number $\mathrm{Re} = lu_l/\nu$ where l, u_l, H_l, μ, σ, ρ and ν are characteristic length, characteristic velocity, externally applied magnetic field intensity, magnetic permeability, electric conductivity, density and kinematic viscosity of the fluid, respectively.

The stream function ψ and the vorticity ω are defined as:

$$u = \frac{\partial \psi}{\partial y}, \qquad v = -\frac{\partial \psi}{\partial x}, \qquad \omega = \frac{\partial v}{\partial x} - \frac{\partial u}{\partial y},$$

respectively [27]. We obtain the stream function equation $\nabla^2\psi = -\omega$. The vorticity equation is derived from the cross-differentiation of Eqs. (2.2) and (2.3) by neglecting the convection terms due to Stokes approximation ($\mathrm{Re} \ll 1$). Thus, the MHD Stokes flow equations are:

$$\nabla^2\psi = -\omega, \tag{2.4}$$

$$\nabla^2\omega = M^2\left(-\frac{\partial u}{\partial y}\sin^2\alpha + \left(\frac{\partial v}{\partial y} - \frac{\partial u}{\partial x}\right)\sin\alpha\cos\alpha + \frac{\partial v}{\partial x}\cos^2\alpha\right) \tag{2.5}$$

with the given boundary conditions in Fig. 1. The unknown vorticity boundary conditions are found by using the method explained in Section 3.

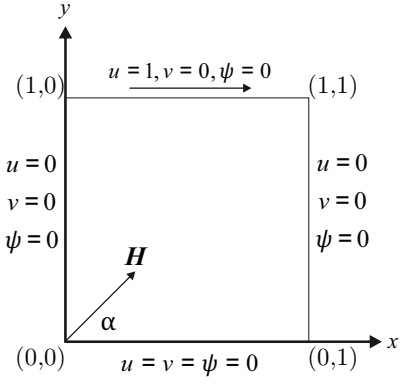

FIG. 1. Problem domain in 2-D (Lid-driven cavity).

3. RBF approximation

In the radial basis function (RBF) approximation method [28], the right hand side function f in the differential equation $\mathcal{L}u(x,y) = f(x,y)$ and the approximate solution u are approximated by RBFs ϕ and Ψ as:

$$f(x,y) \simeq \sum_{i=1}^{n} \beta_i \phi_i(r), \quad (x,y) \in \Omega, \tag{3.1}$$

$$u(x,y) = \sum_{i=1}^{n} \beta_i \Psi_i(r), \tag{3.2}$$

respectively, where $\mathcal{L}$ is a differential operator such that

$$\mathcal{L}\Psi_i(r) = \phi_i(r), \qquad r = \sqrt{(x-x_i)^2 + (y-y_i)^2}$$

is the Euclidean distance, β_i's are the unknown coefficients and n is the number of points. Since the approximate solution u satisfies the boundary condition $\mathcal{B}u = g$ with the boundary operator $\mathcal{B}$ and we get

$$\sum_{i=1}^{n} \beta_i \mathcal{B}\Psi_i(r) = g(x,y), \qquad (x,y) \in \partial\Omega, \tag{3.3}$$

where $\partial\Omega$ is the boundary of the domain Ω. N boundary points and L interior points satisfy Eqs. (3.3) and (3.1), respectively. Thus, the linear system is obtained

$$A\beta = B, \tag{3.4}$$

where

$$A = \begin{bmatrix} \mathcal{B}\Psi_1(r_1) & \mathcal{B}\Psi_2(r_1) & \cdots & \mathcal{B}\Psi_n(r_1) \\ \vdots & \vdots & \ddots & \vdots \\ \mathcal{B}\Psi_1(r_N) & \mathcal{B}\Psi_2(r_N) & \cdots & \mathcal{B}\Psi_n(r_N) \\ \phi_1(r_{N+1}) & \phi_2(r_{N+1}) & \cdots & \phi_n(r_{N+1}) \\ \vdots & \vdots & \ddots & \vdots \\ \phi_1(r_n) & \phi_2(r_n) & \cdots & \phi_n(r_n) \end{bmatrix}_{n\times n}, \qquad \beta = \begin{bmatrix} \beta_1 \\ \vdots \\ \beta_n \end{bmatrix}_{n\times 1},$$

$$B = \begin{bmatrix} g(x_1,y_1) \\ \vdots \\ g(x_N,y_N) \\ f(x_{N+1},y_{N+1}) \\ \vdots \\ f(x_n,y_n) \end{bmatrix}_{n\times 1}.$$

The solution u given in (3.2) is obtained as $u = UA^{-1}B$ since $\beta = A^{-1}B$ where $U_{ij} = \Psi_j(r_i)$, $1 \le i, j \le n$ and it can be reconstructed as $u = G_u + DF$ where $F = \{f_i\}$, $1 \le i \le n$, $G_u = G_1 u_b$ and $D = [\underset{n\times N}{0} \quad \underset{n\times L}{G_2}]$. Here, G_1 and G_2 are the submatrices of UA^{-1} as $UA^{-1} = [\underset{n\times N}{G_1} \quad \underset{n\times L}{G_2}]$, and u_b represents the boundary values of the solution u.

In the literature, there are different types of radial basis functions such as Gaussian $\phi(r) = \exp(c^2 r^2)$, multiquadric (MQ) $\phi(r) = \sqrt{r^2 + c^2}$ and inverse quadratic $\phi(r) = 1/\sqrt{r^2 + c^2}$, where c is the shape parameter. Some studies show that the use of multiquadric RBF gives better results than the others [29–32]. It is observed that the accuracy of the numerical solution depends on the value of the shape parameter. However, a special algorithm is required to determine the optimum value of the shape parameter. In this study, we compared the minimum stream function values for different Hartmann numbers obtained by multiquadric and polynomial radial basis functions in Table 1. The shape parameter is taken as $c = 0.6d/\sqrt{n}$, where d is area of the flow domain and n is total node number [33, 34]. The comparison showed that polynomial results are similar to the results obtained by MQ. Thus, the rest of the computations in this study is carried with the linear polynomial RBF $\phi(r) = 1 + r$, and $\Psi(r) = r^2/4 + r^3/9$ which is obtained from the back substitution $\nabla^2\phi = \Psi$.

Table 1. Iteration numbers and minimum values of ψ for different Hartmann number with $\alpha = 0$.

	$\phi(r) = 1 + r$		$\phi(r) = \sqrt{r^2 + c^2}$	
Hartmann Num.	Iter. Num.	$\psi_{\min}$	Iter. Num.	$\psi_{\min}$
$M = 0$	1486	-1.006414×10^{-1}	1484	-1.003471×10^{-1}
$M = 10$	1487	-7.763441×10^{-2}	1484	-7.730504×10^{-2}
$M = 30$	1489	-5.092238×10^{-2}	1491	-5.055574×10^{-2}
$M = 50$	1492	-4.056662×10^{-2}	1497	-4.017458×10^{-2}

The coupled MHD Stokes equations (2.4)–(2.5) are solved with an iterative procedure.

- $\nabla^2\psi = -\omega$ is solved by using an initial estimate for the vorticity.
- The vorticity boundary condition ω_0 is obtained by using the finite difference method [35]

$$\omega_0 = -\Big(a_0\psi_0 + a_1\psi_p + a_2\psi_q + a_3\psi_n\big|_0\Big),$$

where ψ_0 is the boundary value, ψ_n is the normal derivative of ψ, ψ_p and ψ_q are interior values of stream function at p and q which are ph and qh distances away from the boundary and the coefficients are:

$$a_0 = \frac{-2(p^3 - q^3)}{h^2 p^2 q^2 (p - q)}, \qquad a_1 = \frac{-2q}{h^2 p^2 (p - q)},$$
$$a_2 = \frac{2p}{h^2 q^2 (p - q)}, \qquad a_3 = \frac{-2(p + q)}{hpq}.$$

- The new vorticity value is obtained from Eq. (2.5) with the use of the new values of velocity components which are evaluated from $u = \psi_y$, $v = -\psi_x$.
- The iteration process is terminated when a preassigned tolerance ϵ is reached between two successive iterations

$$\frac{\|\omega^{m+1} - \omega^m\|_\infty}{\|\omega^{m+1}\|_\infty} \leq \epsilon.$$

The derivatives of unknowns are obtained by using the coordinate matrix ϕ ($\phi_{ij} = 1 + r_{ij}$) as $\frac{\partial K}{\partial x} = \frac{\partial \phi}{\partial x}\phi^{-1}K$, $\frac{\partial K}{\partial y} = \frac{\partial \phi}{\partial y}\phi^{-1}K$, where K denotes ω, ψ, u and v.

3.1. Computational procedure for the corner data

The flow in a square cavity is driven by the motion of the top-lid at a speed of $u = 1$ while the other walls are stationary $u = 0$. In order to eliminate the corner singularities, velocity distribution on the top lid of the cavity is applied [36]. Let the boundary value function $u(x)$ be defined by

$$u(x) = \begin{cases} 0.5(1 + \sin(\pi(x - \delta_0/2)/\delta_0)) & 0 \leq x \leq \delta_0, \\ 1 & \delta_0 < x < \delta_1, \\ 0.5(1 + \cos(\pi(x - \delta_1)/\delta_0)) & \delta_1 \leq x \leq 1, \end{cases} \tag{3.5}$$

where δ_0 is a constant and $\delta_1 = 1 - \delta_0$. In this approximation, $u(x)$ is equal to 1 for $x \in [\delta_0, \delta_1]$, and it decreases smoothly at $x \in [0, \delta_0]$ for the left-upper corner, at $x \in [\delta_1, 1]$ for the right-upper corner and is equal to 0 on the vertical walls.

The effect of the velocity distribution on streamlines is checked with the corner eddies. MOFFATT [37] showed the existence of an infinite sequence of loops in decreasing a size for anti-symmetrical Stokes flow between two stationary walls. He also stated that when the fluid is electrically conducting, the reverse flow and eddies form. Figure 2 depicts the streamline patterns and the corner eddies are obtained by using 51×51 uniformly distributed points. Smooth corner eddies are obtained by taking $\delta_0 = 0.05$ comparing the results obtained without velocity distribution. In this study, $\delta_0 = 0.05$ is determined by trial and error. On the other hand, it is also observed that this approximation requires less computational time and the iteration number.

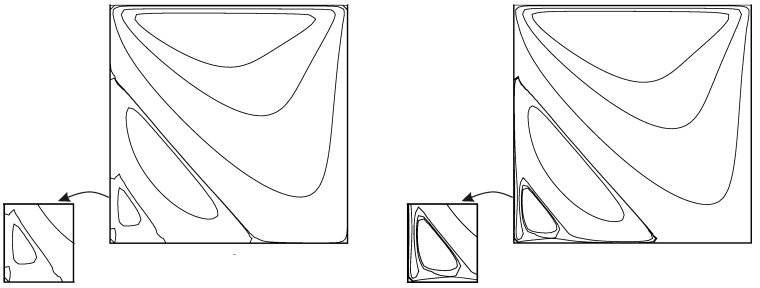

a) b)

FIG. 2. Streamlines at the corner with enlarged portion for $M = 50$ and $\alpha = 3\pi/4$ a) with $\delta_0 = 0.05$, 1488 iterations and 63.394 s CPU time; b) without velocity distribution (3.5), 1605 iterations and 66.593 s CPU time.

4. Numerical results

The present iterative RBF approximation has been applied to the lid-driven square cavity problem under the effect of a uniform applied magnetic field with an angle. Numerical computations are carried out for several values of the moderate Hartmann number ($M \leq 80$) and the inclination angle of magnetic field ($0 \leq \alpha \leq \pi$). The boundary of the square cavity is discretized with $N = 204$ points and $L = 2500$ uniformly distributed interior points are taken, so the number of total points is $n = N + L = 2704$. The preassigned tolerance ϵ is given 10^{-9}. The numerical results are presented in terms of contour plots of a stream function to analyze the behaviour of the Stokes flow.

Firstly, the proposed method is validated by taking $M = 0$, which means that the magnetic field effect on the Stokes flow is neglected. The minimum value of the stream function is found to be -0.1006 which is similar to the result

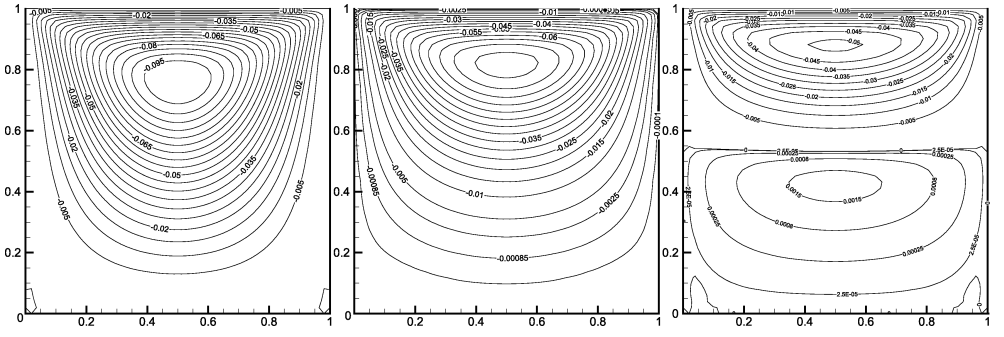

$M = 0$ $M = 10$ $M = 30$

FIG. 3. Streamlines for $M = 0, 10, 30$ and $\alpha = 0$.

$\psi_{\min} = -0.1001$ obtained by SHANKAR [36]. Also, streamlines are obtained for $M = 0, 10, 30$ in the case of $\alpha = 0$. Streamlines in Fig. 3 are in good agreement with the ones in [35].

Numerical results shown in Figs. 4–6 are obtained for several values of M and α to analyze the effects of intensity and the direction of the magnetic field on the Stokes flow. In Fig. 4, it is observed that for $M = 10$, there is no significant change in the streamlines as α increases since the electromagnetic influence on the flow is small. In the case of $\alpha = 0$, as M increases, the center of the main vortex of the flow is close to the top wall due to the impacts of the direction of the magnetic field and the movement of the lid. The retardation effect of the magnetic force causes the formation of new counter rotating vortices under the main vortex. It is shown that as the inclination angle increases, the symmetric distribution of streamlines at $x = 0.5$ is deformed. Vortices are formed at the lower right corner.

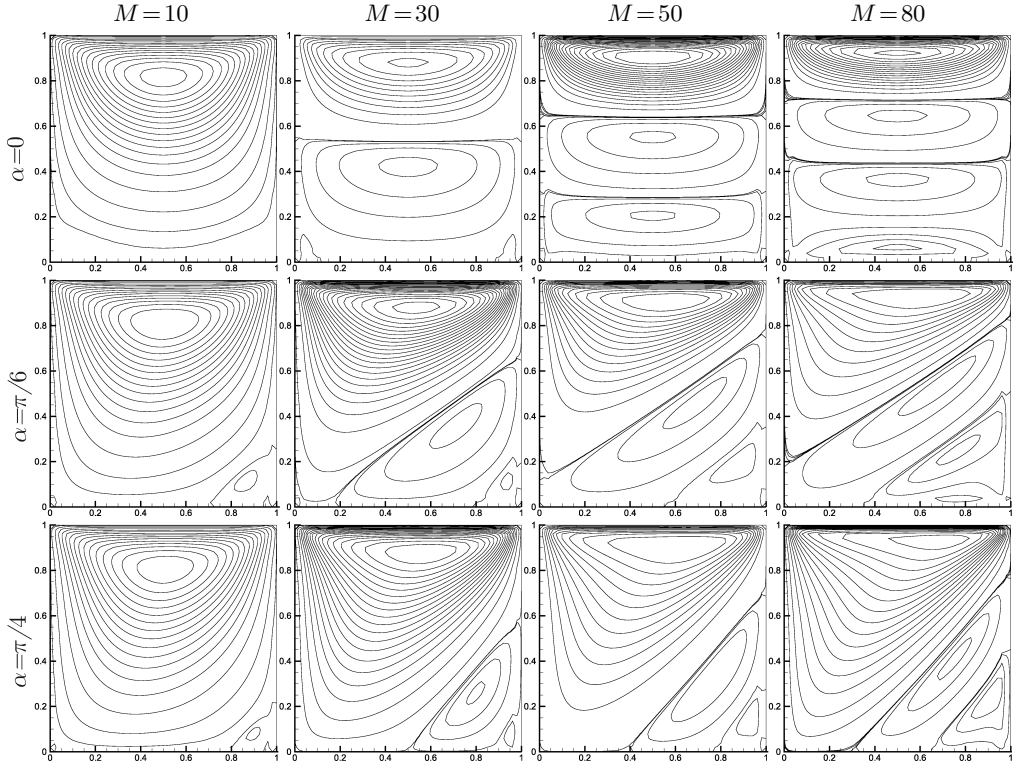

FIG. 4. Streamlines for $M = 10, 30, 50, 80$ and $\alpha = 0, \pi/6, \pi/4$.

Figure 5 depicts the results obtained by taking $\alpha \geq \pi/3$ and $M \geq 10$. An increase in the inclination angle diminishes the size and the number of the vortices. As the angle increases to $\pi/2$, streamlines attain symmetric distribution

at $x = 0.5$ and the vortices at the right lower corner disappear. The reason is that the magnetic force (Lorentz force) suppresses the velocity in the direction perpendicular to the magnetic filed.

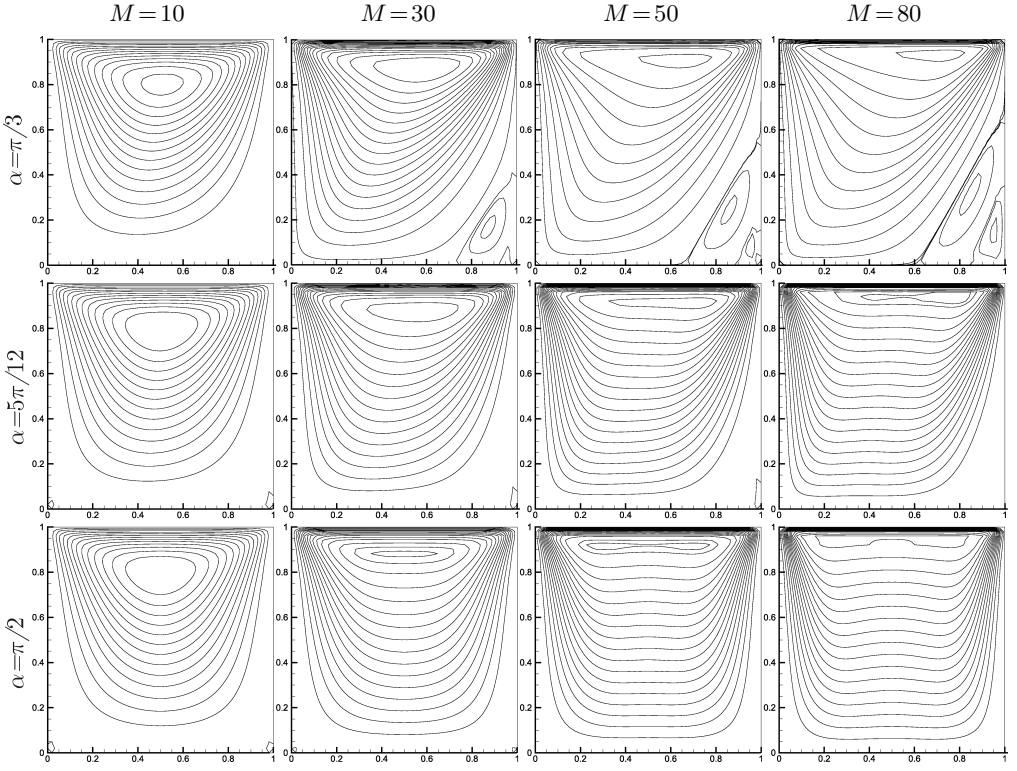

FIG. 5. Streamlines for $M = 10, 30, 50, 80$ and $\alpha = \pi/3, 5\pi/12, \pi/2$.

The stream function contours are obtained for the obtuse angles of the magnetic field ($7\pi/12 \leq \alpha \leq \pi$) in Fig. 6. When α reaches to $2\pi/3$, secondary vortex occurs at the lower left corner. The number of vortices increases with an increase in the inclination angle. The center of the main vortex moves to left upper corner which shows that inclination angle diminishes the effect of the movement of the lid. When α reaches to π, the same flow structure is obtained as in the case of $\alpha = 0$. When we compare Fig. 5 and Fig. 6, the effect of the inclination angle of the magnetic field on the flow is the same because these angles are the supplementary angles. Only difference is observed for the location of vortices. Acute angles cause the formation of the secondary vortex at the right corner. On the other hand, the secondary vortex occurs at the left corner when $\alpha > \pi/2$. It is deduced that flow structure depends on the strength and the orientation of the magnetic field.

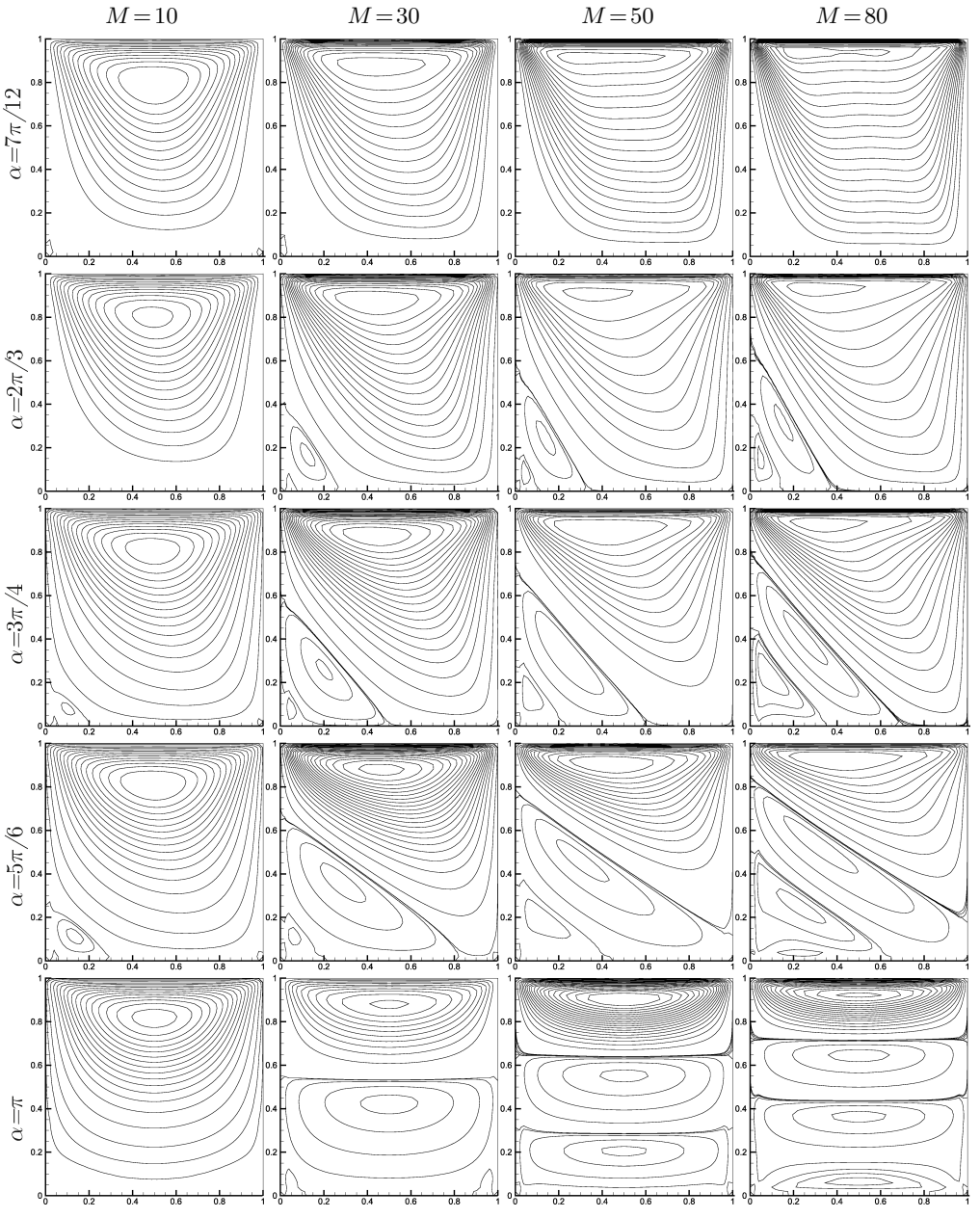

FIG. 6. Streamlines for $M = 10, 30, 50, 80$ and $\alpha = 7\pi/12, 2\pi/3, 3\pi/4, 5\pi/6, \pi$.

In Fig. 7a, the maximum value of $|\psi|$ is plotted for several values $0 \leq M \leq 80$ and $0 \leq \alpha \leq \pi/2$. It is found that as M increases, the magnitude of stream function decreases which is the retardation effect of MHD flow. For a fixed Hartmann

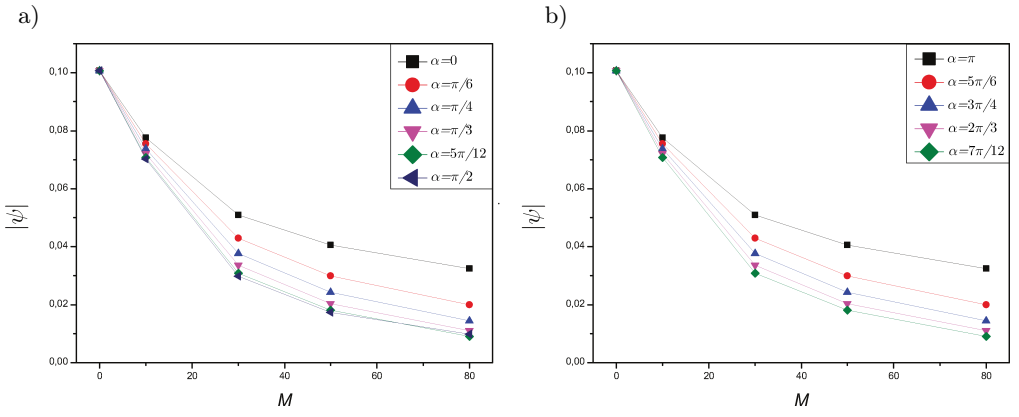

FIG. 7. Maximum value of $|\psi|$ for $M = 0, 10, 30, 50, 80$ with a) $\alpha = 0, \pi/6, \pi/4, \pi/3, 5\pi/12, \pi/2$; b) $\alpha = 7\pi/12, 2\pi/3, 3\pi/4, 5\pi/6, \pi$.

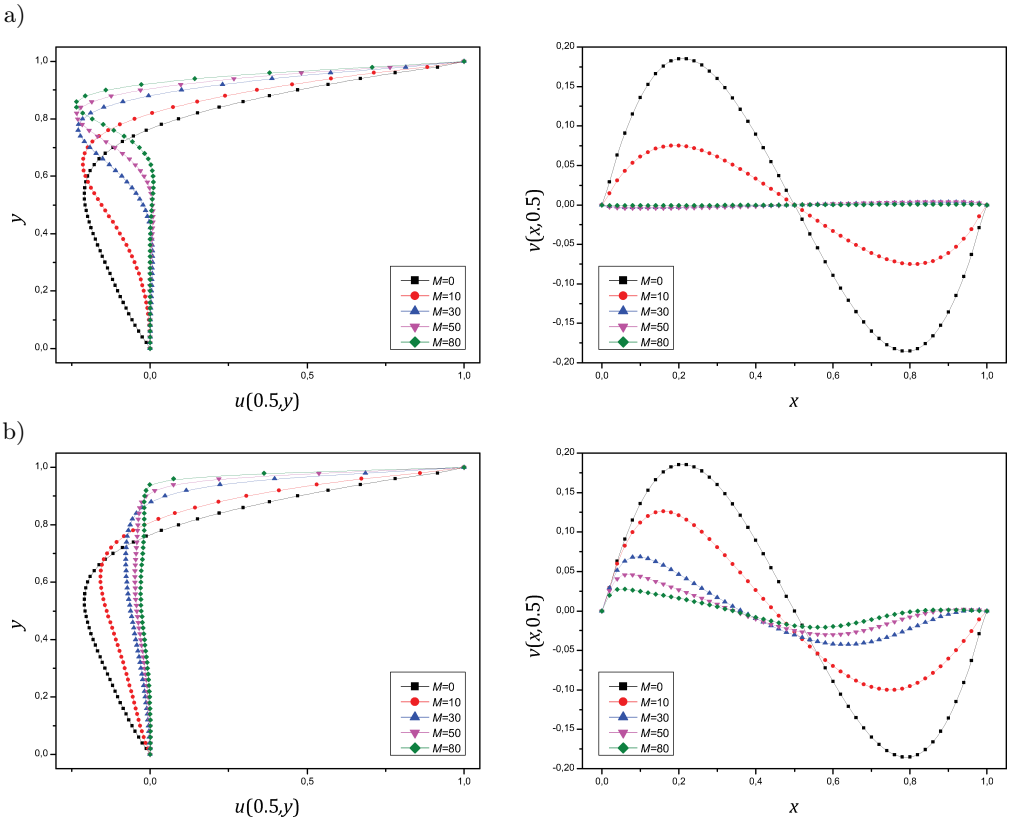

FIG. 8. Hartmann effects on velocity profiles along mid-points in the cavity with 50×50 grid size; a) inclination angle $\alpha = 0$, b) inclination angle $\alpha = \pi/4$.

number, an increase in the inclination angle decreases the magnitude of a stream function. It is deduced that an inclination angle accelerates the decrease in the values of a stream function.

Figure 7b shows the maximum value of the stream function for different values of M and the obtuse angle α. As the inclination angle increases, the magnitude of the stream function increases. Comparing to the results in Fig. 7a, it is observed that stream function takes the same maximum value at α and $\pi - \alpha$ for a fixed Hartmann number since the magnetic force is the same for the supplementary angles.

Figure 8 indicates the impact of the Hartmann number on the centerline velocities for $\alpha = 0$ and $\alpha = \pi/4$. In both cases, an increase in M decreases the velocity values. As the strength of the horizontal magnetic field increases, v-velocity profile is flattened. Since the magnetic force produces resistance in the opposite direction to the velocity perpendicular to the magnetic field. However, the inclination angle weakens the flattening tendency on v-profile.

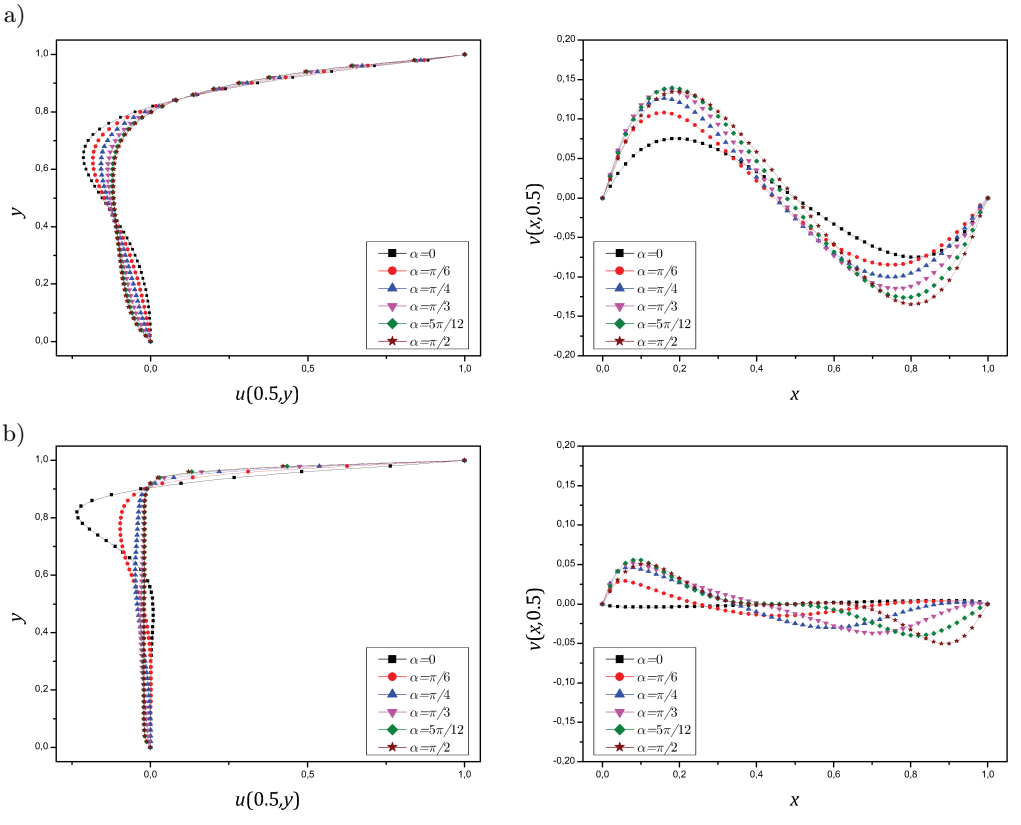

FIG. 9. Inclination angle effects on velocity profiles along mid-points in the cavity with 50×50 grid size; a) $M = 10$, b) $M = 50$.

In Fig. 9, velocity profiles along mid-points are shown for different orientation of the magnetic field and $M = 10, 50$. It is also found that v-centerline velocity attains a minimum value at $\alpha = \pi/2$ regardless of the Hartmann number values. For $M = 50$, the values of u-velocity component are almost zero at the mid-section of the cavity with an increase in α due to the deceleration effect of the magnetic field. The effect of the movement of the lid is observed regardless of the direction of the magnetic field. As the inclination angle increases, v-velocity profiles fluctuate. However, the velocity component in the y-direction is flattened at the center of the cavity for $\alpha \geq 5\pi/12$.

5. Conclusion

The Stokes flow in a lid-driven cavity is simulated in the presence of an applied uniform magnetic field with an inclination angle for the first time in this paper. RBF approximation is employed to MHD Stokes flow equations for different values of the Hartmann number and the inclination angle of the magnetic field. In order to obtain smooth corner eddies, velocity distribution is used for the moving top lid. We observed that an increase in the Hartmann number decreases the magnitude of a stream function regardless of the direction of the magnetic field. As the inclination angle increases in the range $[0, \pi/2]$, the magnitude of the stream function decreases. However, the increase in α, which is in the range $[\pi/2, \pi]$, increases the magnitude of ψ. The formation of the vortices depends on α and M which indicates that both the inclination angle and the strength of the magnetic field control the structure of the flow.

References

1. U. MÜLLER, M. BÜHLER, *Magnetofluiddynamics in Channels and Containers*, Springer, New York, 2001.

2. M. TEZER-SEZGIN, S.H. AYDIN, *Dual reciprocity boundary element method for magnetohydrodynamic flow using radial basis functions*, International Journal of Computational Fluid Dynamics, **16**, 49–63, 2002.

3. M. TEZER-SEZGIN, S.H. AYDIN, *Solution of magnetohydrodynamic flow problems using the boundary element method*, Engineering Analysis with Boundary Elements, **30**, 411–418, 2006.

4. C. BOZKAYA, M. TEZER-SEZGIN, *Fundamental solution for coupled magnetohydrodynamic flow equations*, Journal of Computational and Applied Mathematics, **203**, 125–144, 2007.

5. S. MOLOKOV, *Fully developed liquid-metal flow in multiple rectangular ducts in a strong uniform magnetic field*, European Journal of Mechanics B/Fluids, **12**, 769–787, 1993.

6. X. XIAO, C.N. KIM, *Effects of the magnetic field direction and of the cross-sectional aspect ratio on the mass flow rate of MHD duct flows*, Fusion Engineering and Design, **151**, 2020.

7. T.Q. HUA, J.S. WALKER, *MHD Flow in rectangular ducts with inclined non-uniform tranverse magnetic field*, Fusion Engineering and Design, **27**, 703–710, 1995.
8. M.P. JEYANTHI, S. GANESH, *Numerical solution of steady MHD duct flow in a square annulus duct under strong transverse magnetic field*, International Journal of Ambient Energy, **43**, 1, 2816–2823, 2020.
9. G.H.R. KEFAYATI, M. GORJI-BANDPY, H. SAJJADI, D.D. GANJI, *Lattice Boltzmann simulation of MHD mixed convection in a lid-driven square cavity with linearly heated Wall*, Scientia Iranica, Transactions B: Mechanical Engineering, **19**, 1053–1065, 2012.
10. K. JIN, S.P. VANKA, B.G. THOMAS, *Three-dimensional flow in a driven cavity subjected to an external magnetic field*, ASME Jounal of Fluids Engineering, **137**, 071104, 2015.
11. P.X. YU, J.X. QIU, Q. QIN, ZHEN F. TIAN, *Numerical investigation of natural convection in a rectangular cavity under different directions of uniform magnetic field*, International Journal of Heat and Mass Transfer, **67**, 1131–1144, 2013.
12. S. HUSSAIN, H.F. ÖZTOP, K. MEHMOOD, N. ABU-HAMDEH, *Effects of inclined magnetic field on mixed convection in a nanofluid filled double lid-driven cavity with volumetric heat generation or absorption using finite element method*, Chinese Journal of Physics, **56**, 484–501, 2018.
13. C.C. CHO, *Mixed convection heat transfer and entropy generation of Cu-water nanofluid in wavy-wall lid-driven cavity in presence of inclined magnetic field*, International Journal of Mechanical Sciences, **151**, 703–714, 2019.
14. S. HUSSAIN, M. JAMAL, B.P. GERIDONMEZ, *Impact of fins and inclined magnetic field in double lid-driven cavity with Cu-water nanofluid*, International Journal of Thermal Sciences, **161**, 106707, 2021.
15. D.L. YOUNG, C.W. CHEN, C.M. FAN, K. MURUGESAN, C.C. TSAI, *The method of fundamental solutions for Stokes flow in a rectangular cavity with cylinders*, European Journal of Mechanics B/Fluids, **24**, 703–716, 2005.
16. C.W. CHEN, D.L. YOUNG, C.C. TSAI, K. MURUGESAN, *The method of fundamental solutions for inverse 2D Stokes problems*, Computational Mechanics, **37**, 2–14, 2005.
17. D.L. YOUNG, S.J. JANE, C.M. FAN, K. MURUGESAN, C.C. TSAI, *The method of fundamental solutions for 2D and 3D Stokes problems*, Journal of Computational Physics, **211**, 1–8, 2006.
18. T.I. ELDHO, D.L. YOUNG, *Solution of Stokes flow problem using dual reciprocity boundary element method*, Journal of the Chinese Institute of Engineers, **24**, 141–150, 2001.
19. C.A. BUSTAMANTE, H. POWER, Y.H. SUA, W.F. FLOREZ, *A global meshless collocation particular solution method (integrated radial basis function) for two-dimensional Stokes flow problems*, Applied Mathematical Modelling, **37**, 4538–4547, 2013.
20. A. DELICEOĞLU, S.H. AYDIN, *Topological flow structures in an L-shaped cavity with horizontal motion of the upper lid*, Journal of Computational and Applied Mathematics, **259**, part B, 937–943, 2014.
21. E. ÇELIK, M. LUZUM, A. DELICEOĞLU, *Stokes flow in a Z-shaped cavity with moving upper lid*, Karaelmas Science and Engineering Journal, **11**, 1, 12–22, 2021.
22. S. QIAN, H. BAU, *Magneto-hydrodynamics based microfluidics*, Mechanics Research Communications, **36**, 10–21, 2009.

23. H. YOSINOBU, T. KAKUTANI, *Two-dimensional Stokes flow of an electrically conducting fluid in a uniform magnetic field*, Journal of the Physical Society of Japan, **14**, 1433–1444, 1959.

24. M. GÜRBÜZ, M. TEZER-SEZGIN, *MHD Stokes flow and heat transfer in a lid-driven square cavity under horizontal magnetic field*, Mathematical Methods in the Applied Sciences, **41**, 2350–2359, 2018.

25. O. TÜRK, *An MHD Stokes eigenvalue problem and its approximation by a spectral collocation method*, Computers and Mathematics with Applications, **80**, 2045–2056, 2020.

26. M.K. PRASAD, T. BUCHA, *Magnetohydrodynamic effect on axisymmetric Stokes flow past a weakly permeable spheroid with a solid core*, Archives of Mechanics, **73**, 599–633, 2021.

27. D.J. TRITTON, *Physical Fluid Dynamics*, 2nd ed., Oxford Science Publications, New York, 1988.

28. C.S. CHEN, C.M. FAN, P.H. WEN, *The method of approximate particular solutions for solving certain partial differential equations*, Numerical Methods Partial Differential Equations, **28**, 506–522, 2012.

29. P.P. CHINCHAPATNAM, K. DJIDJELI, P.B. NAIR, *Unsymmetric and symmetric meshless schemes for the unsteady convection-diffusion equation*, Computer Methods in Applied Mechanics and Engineering, **195**, 19–22, 2432–2453, 2006.

30. H. POWER, V. BARRACO, *A Comparison analysis between unsymmetric and symmetric radial basis function collocation methods for the numerical solution of partial differential equations*, Computers and Mathematics with Applications, **43**, 3–5, 551–583, 2002.

31. E. LARSSON, E., B. FORNBERG, *A numerical study of some radial basis function based solution methods for elliptic PDEs*, Computers and Mathematics with Applications, **46**, 5–6, 891–902, 2003.

32. PHANI P. CHINCHAPATNAM , K. DJIDJELI, P.B. NAIR, *Radial basis function meshless method for the steady incompressible Navier–Stokes equations*, International Journal of Computer Mathematics, **84**, 10, 1509-1521, 2007.

33. R. FRANKE, *Scattered data interpolation: tests of some method*, Mathematics of Computation, **38**, 157, 181–200, 1982.

34. J.G. WANGA, G.R. LIU, *On the optimal shape parameters of radial basis functions used for 2-D meshless methods*, Computer Methods in Applied and Mechanical Engineering, **191**, 2611–2630, 2002.

35. M. GÜRBÜZ, M. TEZER-SEZGIN, *MHD Stokes flow in lid-driven cavity and backward-facing step channel*, European Journal of Computational Mechanics, **24**, 279–301, 2015.

36. P.N. SHANKAR, *Slow Viscous Flows: Qualitative Features and Quantitative Analysis Using Complex Eigenfunction Expansions*, Imperial College Press Publisher, London, 2007.

37. H.K. MOFFATT, *Viscous and resistive eddies near a sharp corner*, Journal of Fluid Mechanics, **18**, 1, 1–18, 1964.

Received March 9, 2022; revised version June 29, 2022.
Published online December 9, 2022.